1968-05

Investigation of the non-linear characteristics of fluid-suspended vehicles

Kiessel, Richard Joseph

Massachusetts Institute of Technology

http://hdl.handle.net/10945/12453

INVESTIGATION OF THE NON-LINEAR CHARACTERISTICS OF FLUID-SUSPENDED VEHICLES

by

RICHARD JOSEPH KIESSEL

THESIS SUPERVISOR: H. H. RICHARDSON

MAY 17, 1968

INVESTIGATION OF THE NON-LINEAR CHARACTERISTICS OF FLUID-SUSPENDED VEHICLES

by

RICHARD JOSEPH KIESSEL

B.S., United States Coast Guard Academy

(1962)

Submitted in Partial Fulfillment of the
Requirements for the Degree of
Naval Engineer and the Degree of
Master of Science in Mechanical Engineering
at the
MASSACHUSETTS INSTITUTE OF TECHNOLOGY
May, 1968

Signature of Author: ____________________
Department of Naval Architecture and Marine Engineering, May 17, 1968

Certified by: ____________________
Thesis Supervisor

Certified by: ____________________
Departmental Reader

Accepted by: ____________________
Chairman, Departmental Committee on Graduate Students

INVESTIGATION OF THE NON-LINEAR CHARACTERISTICS OF FLUID-SUSPENDED VEHICLES

by

RICHARD JOSEPH KIESSEL

Submitted to the Department of Naval Architecture and Marine Engineering on May 17, 1968, in partial fulfillment of the requirements for the Master of Science Degree in Mechanical Engineering and the Professional Degree, Naval Engineer.

ABSTRACT

Using present linear theory results for a rigid simple plenum fluid-suspension system, it was possible to determine the accuracy of a non-linear model and of analog computer simulation when using small perturbation amplitudes.

By increasing the perturbation amplitudes it was possible to show that the range of validity of the linear theory solution increased as the lead time constant increased and also as the lead-to-lag time constant ratio increased.

Further increasing of the perturbation amplitude showed that the maximum allowable perturbation amplitude increased as the lead time constant increased and also as the lead-to-lag time constant ratio increased.

Increasing the perturbation amplitude beyond the range of validity of the linear theory showed that the peak dimensionless acceleration and the peak dimensionless change in vehicle-suspension-guideway clearance decreased.

Thesis Supervisor: H. H. Richardson
Associate Professor of Mechanical Engineering

TABLE OF CONTENTS

Title Page i

Abstract ii

Table of Contents iii

List of Figures iv

Nomenclature v

Introduction 1

Procedure 12

Results and Discussion 13

Conclusions and Recommendations 20

Appendix

Detailed Precedure

Development of Non-Linear Model 22

Development of the Analog Computer Simulation 28

Determination of Data Points 31

Summary of Data 34

Sample Calculation 37

Bibliography 40

LIST OF FIGURES

1. Schematic Diagram of Simple Rigid Plenum Suspension 3

2. Fluid-Suspension Vehicle Moving at Velocity "v" over a Guideway with Average Distance between Perturbations of "λ" 7

3. Linear Theory Dimensionless Optimum Lag Time Constant, Dimensionless Peak Acceleration, and Dimensionless Peak Change in Vehicle-Suspension-Guideway Clearance Versus Dimensionless Lead Time Constant 10

4. Peak Dimensionless Vertical Acceleration Versus Lead Time Constant and Dimensionless Perturbation Height for Optimum Lag Time Constant 14

5. Peak Dimensionless Change in Vehicle-Suspension-Guideway Clearance Versus Lead Time Constant and Dimensionless Perturbation Height for Optimum Lag Time Constant 15

6. Peak Dimensionless Vertical Acceleration Versus Lead-to-Lag Time Constant Ratio and Dimensionless Perturbation Height 16

7. Peak Dimensionless Change in Vehicle-Suspension-Guideway Clearance Versus Lead-to-Lag Time Constant Ratio and Dimensionless Perturbation Height 17

8. Operational Block Diagram of a Simple Rigid Plenum Suspension Assuming a Unity Voltage Scaling Factor 29

NOMENCLATURE

A	Suspension base area
A_s	Supply area
$\bar{A}$	Dimensionless equilibrium active volume, Ah_e/V_{ce}
$/A$	Dimensionless acceleration, $\lvert \ddot{y}_2 \rvert / \omega_n^2 y_o$
$/A_p$	Peak dimensionless acceleration
C_d	Discharge coefficient
F	Suspension force
g	Acceleration of gravity
$\lvert H$	Dimensionless change in vehicle-suspension-guideway clearance, $\lvert h-h_e \rvert / y_o$
$\lvert H_p$	Peak dimensionless change in vehicle-suspension-guideway clearance
h	Vehicle-suspension-guideway clearance, y_2-y_o
K_s	Static suspension stiffness
l	Peripheral length of skirt or sealing region
m	Vehicle mass per suspension pad
p	Absolute pressure
s	Laplace transform operator
V	Volume
V_o	Cushion dead volume, V_c-Ah_e
v	Vehicle's forward velocity

w	Mass flow rate
$\bar{w}_e$	Flow ratio, $w_e/\rho_{ce}V_{ce}$
y_2	Vehicle displacement
y_o	Guideway displacement
γ	Polytropic exponent
Δ	Denotes a small change
δF	Increment in force that suspension can support in addition to equilibrium load
λ	Average distance between disturbances
ρ	Density
τ_1	Lead time constant
τ_2	Lag time constant
τ_1'	Dimensionless lead time constant, $\tau_1\omega_n$
τ_2'	Dimensionless lag time constant, $\tau_2\omega_n$
ω_n	Natural frequency, $\sqrt{K_s/m}$
ω'	Dimensionless frequency, ω/ω_n

Subscripts

a	Ambient
c	Cushion region
e	Equilibrium
s	Supply

Superscripts

•	Denotes time derivative
—	Denotes dimensionless value obtained by dividing by the equilibrium value (unless noted above)

INTRODUCTION

Throughout his history, man has continually strived to move himself and his goods from one place to another with ever-increasing speed. The horse, ship, railroad train, automobile, and airplane all offered increases in speed and were, therefore, readily accepted.

We have now, however, reached a paradox in the field of short haul (up to distances of four to six hundred miles) transportation. The fastest mode of transportation is often in reality the most time consuming. This is the result of congestion at airports, and the advent of the "super-jets" and "air-busses" will only compound the problem. An alternate solution involving smaller, but more frequent, aircraft merely moves the congestion from the terminal building to the runway, also increasing costs as a result of the decreased payload to gross weight ratio.

Efforts to increase the speed of the surface transportation modes have thus been attempted in many areas of the world. These efforts have, however, pointed up two major limitations: mechanical suspension deficiencies and high power requirements.

The suspension deficiencies are of prime importance as these, coupled with road-bed irregularities, produce intolerable accelerations and heave motions at speeds of two to three hundred miles per hour. Efforts to reduce the road-bed irregularities have

proven to be both expensive and of short duration because of uneven loading and settling. Also, the limit appears to have been reached in the design of mechanical suspension systems with no major break-throughs expected in the near future.

With these limitations in mind, it was decided to attempt a fresh approach to the suspension system for a high-speed ground transportation vehicle. The result of this new approach was the fluid-suspended vehicle. A form of this type of suspension is shown schematically in figure one (1). As shown, the vehicle does not make physical contact with the guideway, but rather, floats on a cushion of compressed air. It is this cushion of air which gives the suspension its dynamic characteristics. This cushion of air acts as a spring with its corresponding lead time constant and also acts to impart a lag time constant, as will be shown later.

This fluid-suspension system suggests advantages over the mechanical suspension in the consequent financial savings in guideway construction. Through the use of low pressure air, of approximately one pound per square inch, gauge, the high unit loadings encountered in the mechanical suspension can be eliminated, thus prolonging guideway life. Also, locally rough materials, such as concrete, may be used as the guideway material since there are no wheels or tires to wear out.

One disadvantage of the mechanical suspension cited

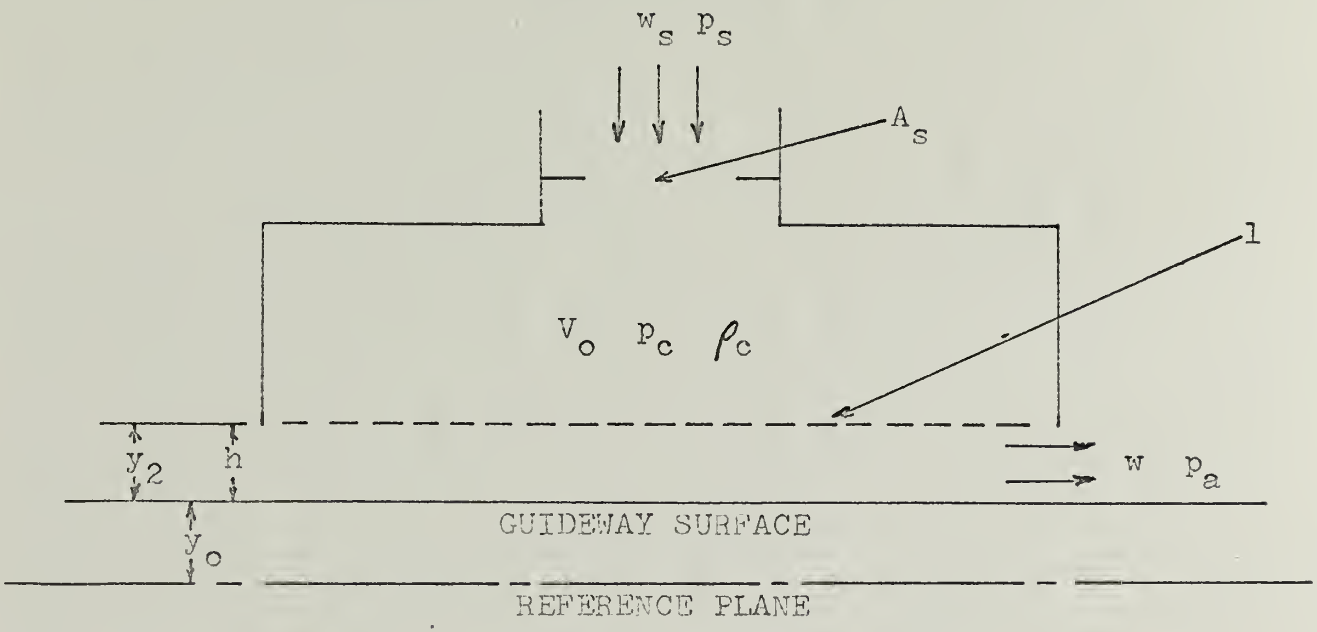

FIGURE 1, Schematic Diagram of Simple Rigid Plenum Suspension

above is the high power requirement necessary to overcome wind drag on the vehicle. This power requirement is still present with the use of a fluid suspension and is, in fact, augmented by the power required to support the vehicle. At the high operating speeds envisioned, however, this hovering power is expected to be small compared with the total power requirements. At these speeds the weight of the vehicle could conceivably be supported by compressed air provided either by aerodynamic means or by induction of air from the stagnation region at the front of the vehicle. In this way the hover-power requirements could be reduced and thus the total power requirement would approach that of a mechanically-suspended vehicle.

Because of the anticipated advantages of a fluid-suspended vehicle, a linearized model was formulated to further explore the vehicular dynamics. This exploration was begun by striving to combine the basic equations describing the suspension. These equations included ones describing flow into and out of the cushion, the continuity equation for the cushion volume, Newton's Second Law, and the equation of state of the fluid and are the same as those used for the non-linear model in the Detailed Procedure. The simplest transfer function which can be formed from these equations, assuming the vehicle-suspension-guideway clearance to be equal around the periphery of the cushion, is

$$\frac{\Delta F}{\Delta h} = K_s \frac{\tau_1 s+1}{\tau_2 s+1} \qquad (1)$$

where, for the simple rigid plenum suspension,

$$\Delta F = F-F_e \qquad (2)$$

is the incremental change in suspension force,

$$\Delta h = h-h_e \qquad (3)$$

is the incremental change in the vehicle-suspension-guideway clearance,

$$K_s = \frac{F_e}{h_e} \frac{2}{1+1/\sqrt{\delta F}} \qquad (4)$$

is the static stiffness of the suspension,

$$\tau_1 = \frac{\bar{A}}{\bar{W}_e} \qquad (5)$$

is the lead time constant and physically represents the time a fluid particle spends in the active cushion volume,

$$\tau_2 = \frac{1}{\bar{W}_e} \frac{p_{ce}-p_a}{\gamma p_{ce}} \frac{2}{1+1/\sqrt{\delta F}} \qquad (6)$$

is the lag time constant and physically represents the charging

lag of the entire cushion volume considered as a fluid capacitance,

$$\overline{\delta F} = \frac{p_s - p_{ce}}{p_{ce} - p_a} \tag{7}$$

is the ratio of maximum incremental force which the suspension can carry to the equilibrium force,

$$\bar{A} = \frac{Ah_e}{V_{ce}} \tag{8}$$

is the dimensionless maximum active volume at equilibrium, and

$$\bar{w}_e = \frac{w_e}{\rho_{ce} V_{ce}} \tag{9}$$

is the reciprocal of the time a fluid particle spends in the entire cushion volume at equilibrium.

From data on the distribution of guideway irregularities, both in magnitude and average distance between these perturbations, it is possible to describe the perturbations as a sinusoidal disturbance. This disturbance would have a frequency equal to the vehicle's forward velocity divided by the average distance between perturbations. This would suggest that the transfer function should be solved for sinusoidal disturbances. When this is done, it yields

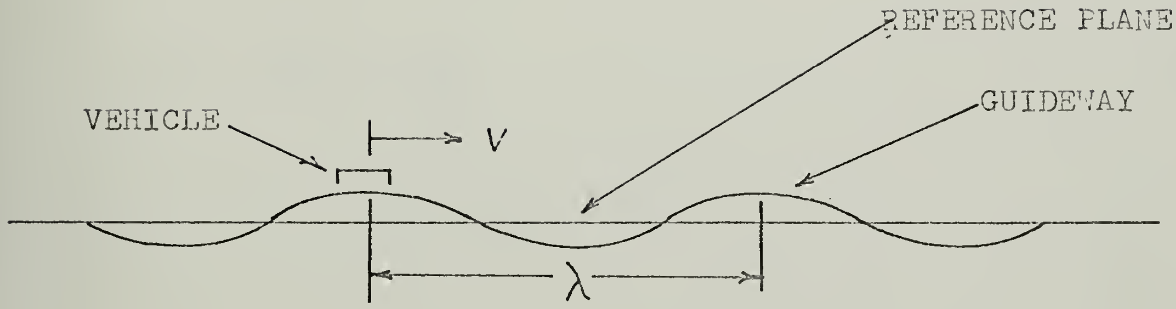

FIGURE 2, Fluid-Suspension Vehicle Moving at Velocity "v" over a Guideway with Average Distance between Perturbations "λ"

$$\mathcal{A} = \frac{|\ddot{y}_2|}{y_o \omega_n} = \frac{\omega'^2 \sqrt{1 + \tau_1'^2 \omega'^2}}{\sqrt{(1 - \omega'^2)^2 + \omega'^2 (\tau_1' - \tau_2' \omega'^2)^2}} \qquad (10)$$

$$\mathcal{H} = \frac{|h - h_e|}{y_o} = \frac{\omega'^2 \sqrt{1 + \tau_2'^2 \omega'^2}}{\sqrt{(1 - \omega'^2)^2 + \omega'^2 (\tau_1' - \tau_2' \omega'^2)^2}} \qquad (11)$$

where

$\mathcal{A}$ = the dimensionless vehicle acceleration

$\mathcal{H}$ = the dimensionless change in vehicle-suspension-guideway clearance

$$\omega' = \frac{\omega}{\omega_n} = \frac{v}{\lambda \omega_n} \qquad (12)$$

is the dimensionless disturbing frequency,

$$\tau_1' = \tau_1 \omega_n \qquad (13)$$

is the dimensionless lead time constant,

$$\tau_2' = \tau_2 \omega_n \qquad (14)$$

is the dimensionless lag time constant, and

$$\omega_n = \sqrt{\frac{k_s}{m}} = \sqrt{\frac{g}{h_e}} \sqrt{\frac{2}{1 + 1/\delta F}} \qquad (15)$$

is the natural frequency of the suspension.

The solution of the dimensionless acceleration shows that peak values occur at or near the natural frequency of the vehicle and at very large frequencies when the dimensionless lead time constant is less than one. By equating these two peak values, an optimum lag time constant can be obtained as a function of the lead time constant.

$$/A_p = \frac{\sqrt{1+{\tau'_1}^2}}{\tau'_1 - \tau'_2} = \frac{\tau'_1}{\tau'_2} \tag{16}$$

$$\tau'_2 = \frac{{\tau'_1}^2}{\tau'_1 + \sqrt{1+{\tau'_1}^2}} \tag{17}$$

Using this optimum value of the lag time constant, it is now possible to solve equations ten (10) and eleven (11) for the peak values of the dimensionless vehicle acceleration and dimensionless change in vehicle-suspension-guideway clearance for a particular lead time constant. These solutions are shown graphically in figure three (3). Using this figure and data on the distribution of guideway irregularities, both in magnitude and in average distance between these perturbations, it is now possible to design a fluid-suspension system and

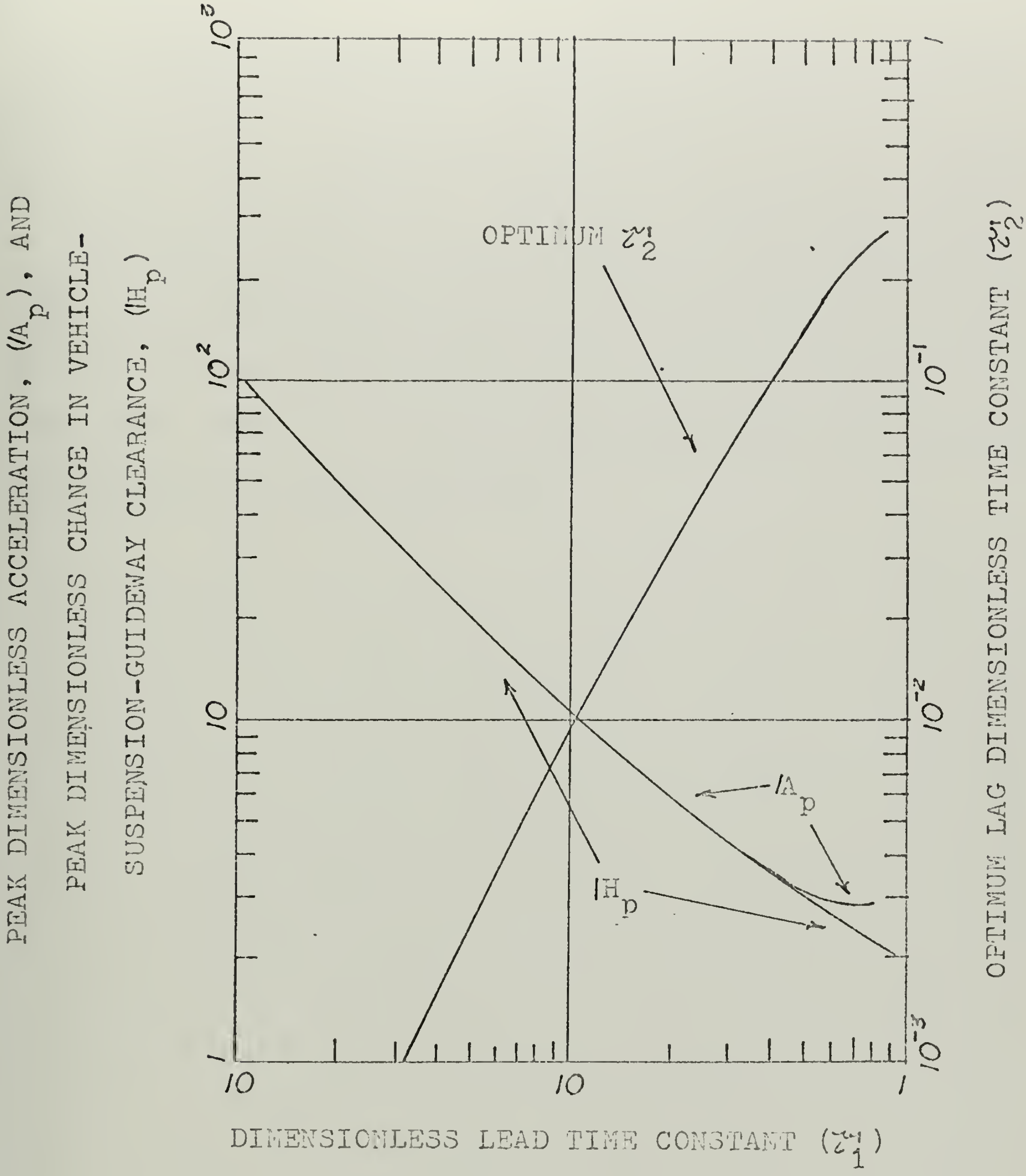
PEAK DIMENSIONLESS ACCELERATION, (A_p), AND
PEAK DIMENSIONLESS CHANGE IN VEHICLE-
SUSPENSION-GUIDEWAY CLEARANCE, (H_p)
10^3
10^2
10
1
OPTIMUM τ'_2
A_p
H_p
1
10^-1
10^-2
10^-3
OPTIMUM LAG DIMENSIONLESS TIME CONSTANT (τ'_2)
10
10
1
DIMENSIONLESS LEAD TIME CONSTANT (τ'_1)

FIGURE 3

determine its dynamic characteristics.

As a result of limitations of linear solutions, however, questions arose as to the range of validity of the solutions and also as to the response of the vehicle beyond this range. It is the purpose of this thesis to answer these questions for the case of a simple rigid plenum fluid-suspended vehicle and to investigate the condition where the lag time constant equals the lead time constant. It is at this point that the linearized transfer function becomes infinite.

PROCEDURE

By using a simple rigid plenum fluid-suspension system, a non-linear mathematical model was formulated and simulated on an analog computer. The details of this formulation and simulation are contained in the DETAILED PROCEDURE. This simulation was then used to determine the maximum acceleration and the maximum change in vehicle-suspension-guideway clearance for a range of lead time constants and their associated optimum lag time constants. By checking these values for small perturbations, the simulation was verified. The perturbation amplitude was then increased until the maximum value allowed by the system was obtained. This occurred either when the vehicle struck the guideway or when the cushion pressure equaled or exceeded the source pressure.

The simulation was then used to determine the maximum acceleration and the maximum change in vehicle-suspension-guideway clearance for the condition of a fixed lead time constant with values of the lag time constant approaching that of the lead time constant.

RESULTS AND DISCUSSION

Figures four (4) and five (5), which contain the results of varying the lead time constant with the optimum lag time constant, show that the peak dimensionless acceleration and the peak dimensionless change in vehicle-suspension-guideway clearance obtained for a dimensionless perturbation height of 0.01 correspond very closely to the linear theory solution for all values of the lead time constant. These variances are probably the result of round-off errors in setting up the problem on the computer.

These figures also show that as the lead time constant is increased, the range of validity of the linear solution increases to a dimensionless perturbation height of 0.2, and the maximum allowable dimensionless perturbation height increases to 0.4.

It is also noted that the peak dimensionless acceleration and the peak dimensionless change in vehicle-suspension-guideway clearance decrease as the dimensionless perturbation height is increased above the linear solution range.

Figures six (6) and seven (7), which contain the results of allowing the lag time constant to approach and equal the lead time constant, show that the peak dimensionless acceleration and peak dimensionless change in vehicle-suspension-guideway clearance obtained for a dimensionless perturbation height of

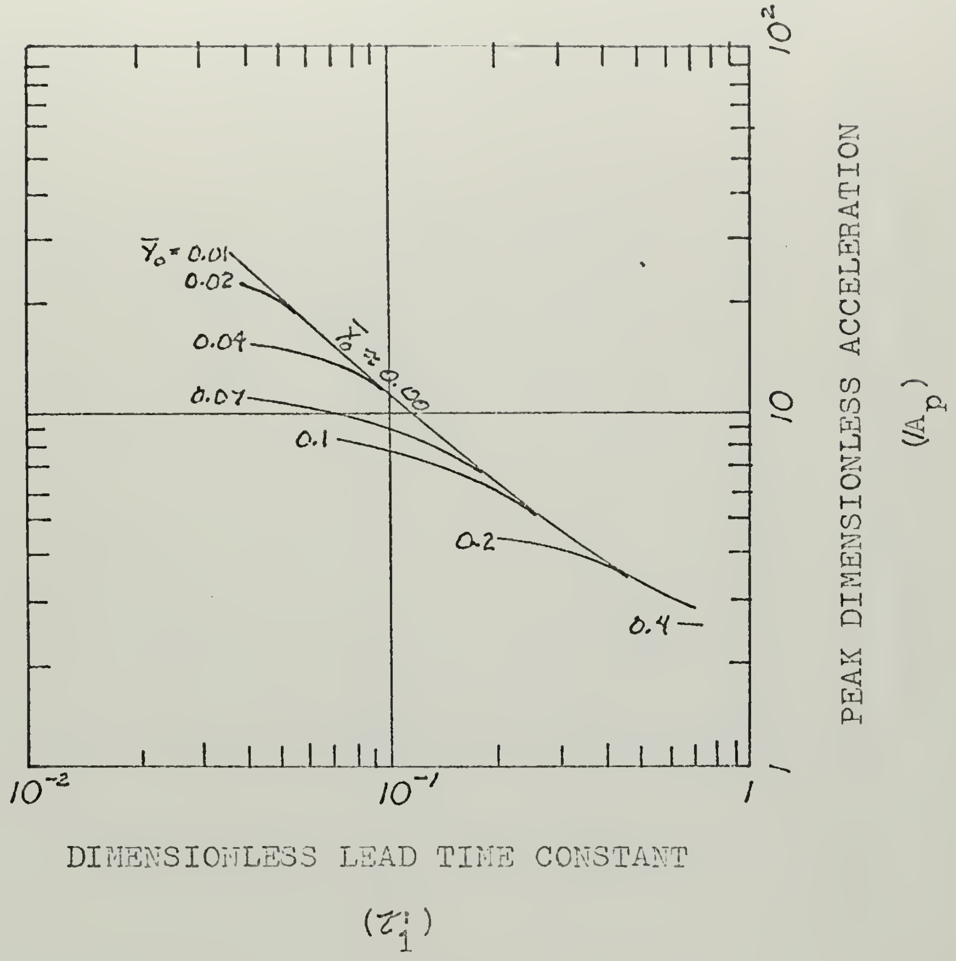

FIGURE 4, Peak Dimensionless Vertical Acceleration Versus Lead Time Constant and Dimensionless Perturbation Height for Optimum Lag Time Constant

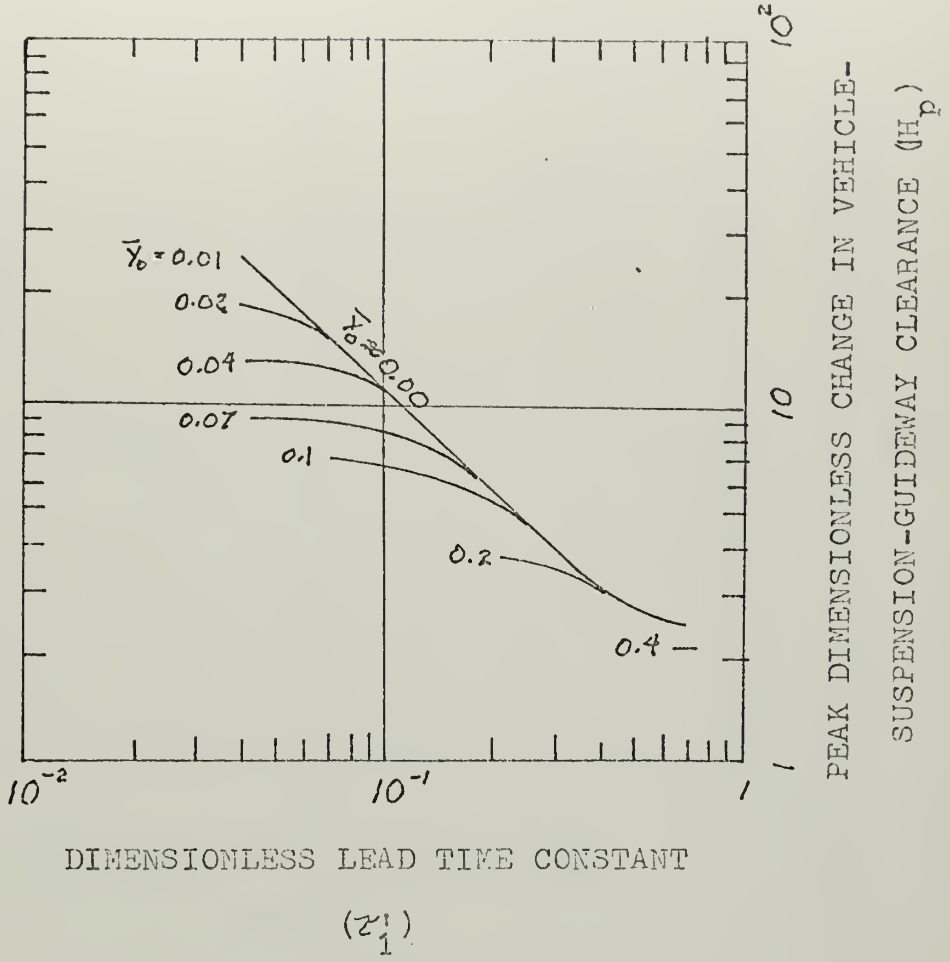

FIGURE 5, Peak Dimensionless Change in Vehicle-Suspension-Guideway Clearance Versus Lead Time Constant and Dimensionless Perturbation Height for Optimum Lag Time Constant

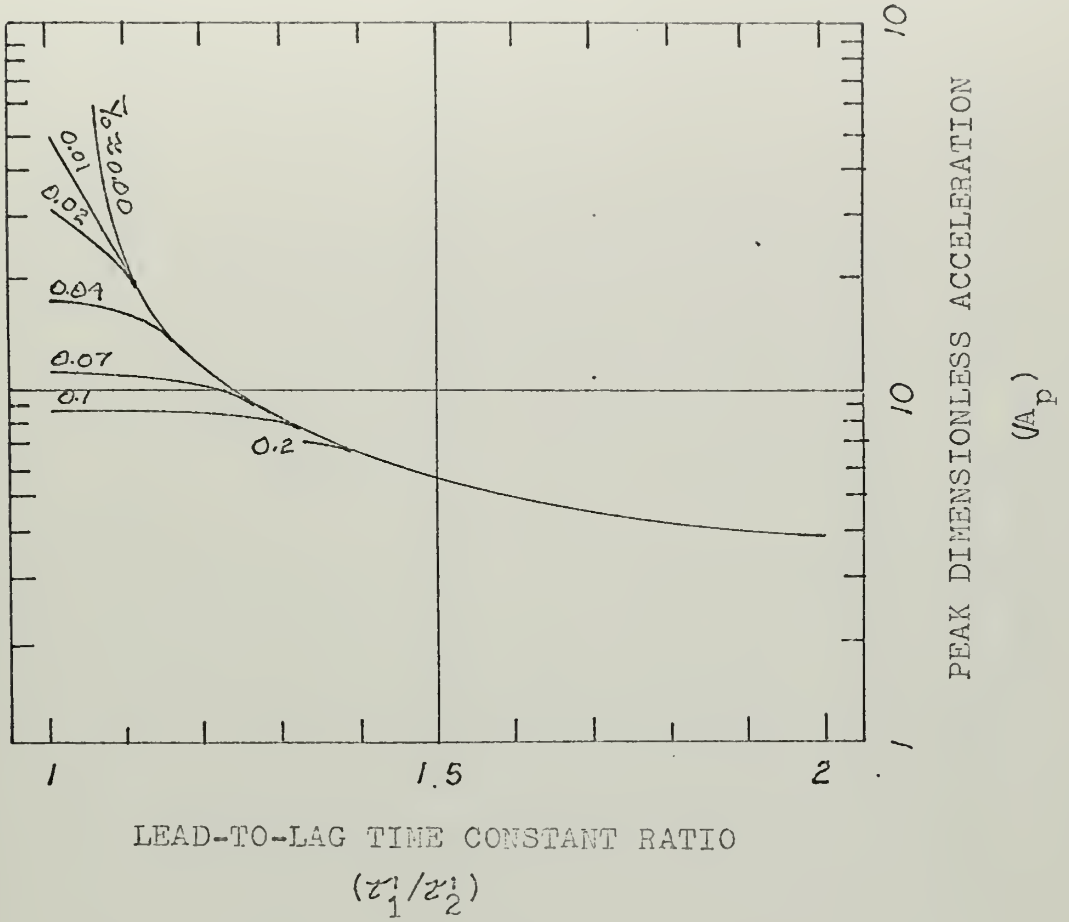

FIGURE 6, Peak Dimensionless Vertical Acceleration Versus Lead-to-Lag Time Constant Ratio and Dimensionless Perturbation Height

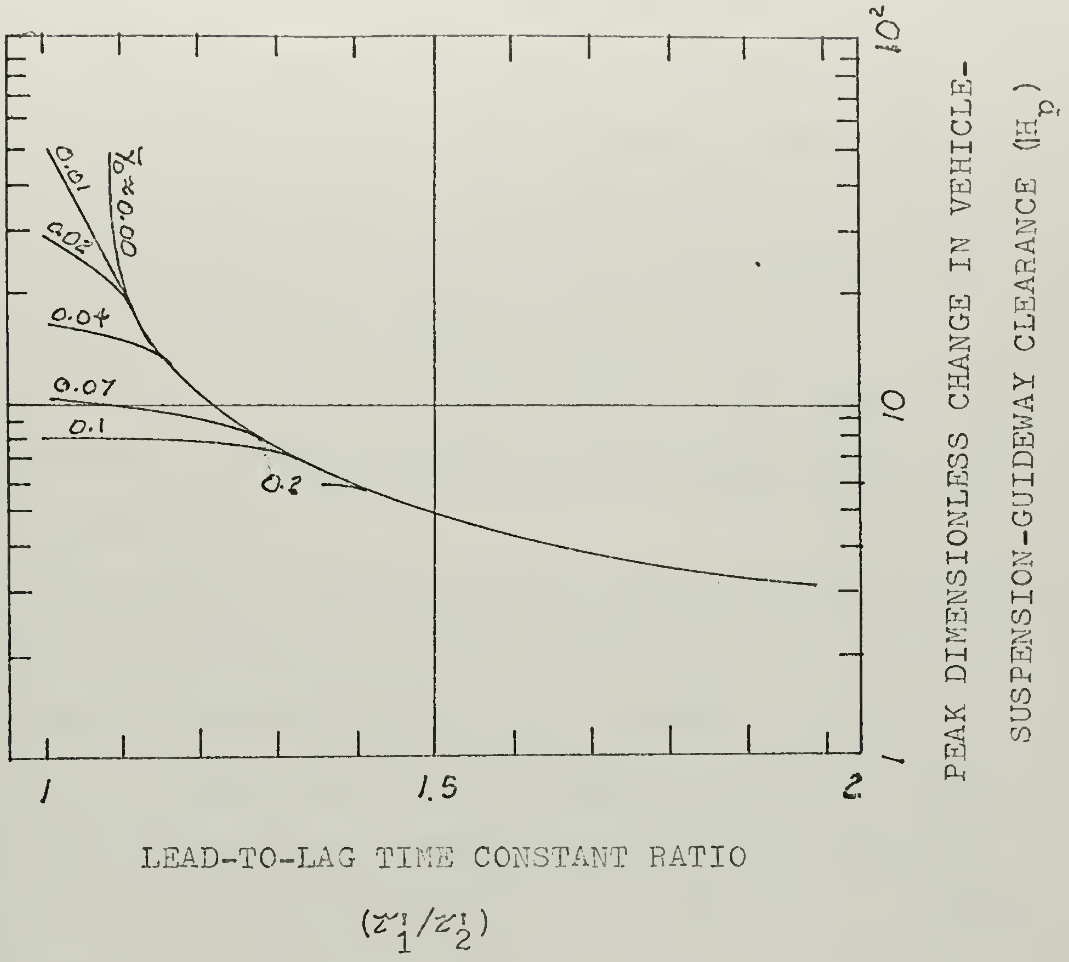

FIGURE 7, Peak Dimensionless Change in Vehicle-Suspension-Guideway Clearance Versus Lead-to-Lag Time Constant Ratio and Dimensionless Perturbation Height

0.01 correspond very closely to the linear solution. There is one exception, however, in the case where the lead and lag time constants are equal. At this point linear theory predicts infinite values. However, the computer showed a finite value for a dimensionless perturbation height of 0.01.

When a disturbance was introduced and then removed, the system continued to oscillate indefinitely with a peak acceleration of 15.36 feet per second squared and a peak change in vehicle-suspension-guideway clearance of 44 per cent of the equilibrium height.

These observations suggest that the linear theory solution is only valid for infinitely small disturbances.

These figures also show that as the lead-to-lag time constant ratio increases to two, the range of validity of the linear solution increases to a dimensionless perturbation height of 0.2 and the maximum dimensionless perturbation height allowed increases to 0.2.

As also noted in the other case, the peak dimensionless acceleration and the peak dimensionless change in vehicle-suspension-guideway clearance decreases as the dimensionless perturbation height is increased above the linear solution range.

The fact that the peak dimensionless acceleration and the peak dimensionless change in vehicle-suspension-guideway clearance decreases for dimensionless perturbation heights

beyond the range of validity of the linear theory solution implies that there is a bias in the system. This bias can be shown quite clearly in the case where the lag time constant equaled the lead time constant and the system oscillated indefinitely at zero perturbation height.

CONCLUSIONS AND RECOMMENDATIONS

1. When the lead time constant is increased using the optimum lag time constant
    a. The range of validity of the linear solution increases
    b. The maximum allowable dimensionless perturbation height increases
2. When the lag time constant is allowed to approach the lead time constant
    a. The range of validity of the linear solution decreases to zero
    b. The maximum allowable dimensionless perturbation height decreases
3. When the dimensionless perturbation height is increased beyond the range of validity of the linear theory, the peak dimensionless acceleration and the peak dimensionless change in vehicle-suspension-guideway clearance decrease.

It is recommended that, when the new Mechanical Engineering Department Analog Computer facilities become available, this model be used as a basis for investigation of the bias noted in the system.

APPENDIX

DETAILED PROCEDURE

DEVELOPMENT OF NON-LINEAR MODEL

The continuity equation for the cushion volume can be written as

$$w_s - w = \dot{\rho}_c\dot{V}_c = \rho_c\dot{V}_c + V_c\dot{\rho}_c \qquad (18)$$

Assuming that the density perturbations are small, this can be nondimensionlized about equilibrium as

$$\bar{w}_e(\bar{w}_s - \bar{w}) = \dot{\bar{V}}_c + \bar{V}_c\dot{\bar{\rho}}_c \qquad (19)$$

where

$$\bar{w}_e = \frac{w_e}{\rho_{ce}V_{ce}} \qquad (9)$$

Since a practical suspension would keep the pressure differences as small as possible, the incompressible flow equation can be used to describe the flows into and out of the cushion volume as

$$w_s = A_sC_{ds}\sqrt{2\rho_{ce}(p_s-p_c)} \qquad (20)$$

$$w = hlC_d\sqrt{2\rho_{ce}(p_c-p_a)} \qquad (21)$$

At equilibrium these flow equations become

$$w_s = w_e = A_s C_{ds}\sqrt{2\rho_{ce}(p_s-p_{ce})} \qquad (22)$$

$$w = w_e = h_e l C_d\sqrt{2\rho_{ce}(p_{ce}-p_a)} \qquad (23)$$

The flow equations can be nondimensionalized by dividing by the equilibrium conditions.

$$\bar{w}_s = \frac{w_s}{w_e} = \sqrt{\frac{p_s-p_c}{p_s-p_{ce}}} \qquad (24)$$

$$\bar{w} = \frac{w}{w_e} = \sqrt{\frac{p_c-p_a}{p_{ce}-p_a}} \qquad (25)$$

Newton's Second Law can be used to equate the cushion pressure and the acceleration of the vehicle as

$$F = A(p_c-p_a) = m(g+\ddot{y}_2) \qquad (26)$$

At equilibrium this becomes

$$F = F_e = A(p_{ce}-p_a) = mg \qquad (27)$$

Nondimensionalizing about equilibrium produces

$$\frac{p_c - p_a}{p_{ce} - p_a} = \frac{g + \ddot{y}_2}{g} = 1 + \frac{\ddot{y}_2}{g} = 1 + \frac{h_e}{g}\,\bar{\ddot{y}}_2 \qquad (28)$$

where

$$\bar{\ddot{y}}_2 = \frac{\ddot{y}_2}{h_e} \qquad (29)$$

Taking the time derivative of the above yields

$$\frac{\dot{p}_c}{p_{ce} - p_a} = \frac{h_e}{g}\,\bar{\dddot{y}}_2 \qquad (30)$$

Combining the above with the flow equations to eliminate the pressure terms produces

$$\bar{w}_s = \sqrt{1 - \frac{1}{\overline{\delta F}}\,\frac{h_e}{g}\,\bar{\ddot{y}}_2} \qquad (31)$$

$$\bar{w} = \sqrt{1 + \frac{h_e}{g}\,\bar{\ddot{y}}_2} \qquad (32)$$

where

$$\overline{\delta F} = \frac{p_s - p_{ce}}{p_{ce} - p_a} \qquad (7)$$

The cushion volume can be written as

$$V_c = V_o + Ah \tag{33}$$

where

$$V_o = V_{ce} - Ah_e \tag{34}$$

is the cushion dead volume.

Dividing by the equilibrium cushion volume to nondimensionalize gives

$$\bar{V}_c = \bar{V}_o + \frac{Ah}{V_{ce}} = V_o + \bar{A}\bar{h} \tag{35}$$

where

$$\bar{A} = \frac{Ah_e}{V_{ce}} \tag{8}$$

$$\bar{h} = \frac{h}{h_e} = \frac{y_2 - y_o}{h_e} \tag{36}$$

Taking the time derivative of the above yields

$$\dot{\bar{V}}_c = \bar{A}\,\dot{\bar{h}} \tag{37}$$

Again assuming the density perturbations are small, and

assuming a polytropic process, the equation of state of the fluid is

$$\frac{\dot{p}_c}{p_{ce}} = \frac{\gamma\dot{\rho}_c}{\rho_{ce}} = \gamma\dot{\bar{\rho}}_c \tag{38}$$

Combining with equation thirty (30), the above becomes

$$\dot{\bar{\rho}}_c = \frac{p_{ce}-p_a}{\gamma p_{ce}}\,\frac{h_e}{g}\,\dddot{\bar{y}}_2 \tag{39}$$

Substituting the above expressions into equation nineteen (19), the final form of the non-linear mathematical model is

$$\bar{w}_e\sqrt{1-\frac{1}{\overline{\delta F}}\,\frac{h_e}{g}\,\ddot{\bar{y}}_2} \;-\; \bar{w}_e\bar{h}\sqrt{1+\frac{h_e}{g}\,\ddot{\bar{y}}_2}$$

$$= \bar{A}\,\dot{\bar{h}} + (\bar{V}_o+\bar{A}\,\bar{h})\,\frac{p_{ce}-p_a}{\gamma p_{ce}}\,\frac{h_e}{g}\,\dddot{\bar{y}}_2 \tag{40}$$

where

$$\bar{w}_e = \frac{w_e}{\rho_{ce}V_{ce}} \tag{9}$$

$$\overline{\delta F} = \frac{p_s-p_{ce}}{p_{ce}-p_a} \tag{7}$$

$$\ddot{\bar{y}}_2 = \frac{\ddot{y}_2}{h_e} \tag{29}$$

$$\bar{h} = \frac{h}{h_e} = \frac{y_2 - y_o}{h_e} \tag{36}$$

$$\bar{A} = \frac{Ah_e}{V_{ce}} \tag{8}$$

DEVELOPMENT OF THE ANALOG COMPUTER SIMULATION

The analog computer used for this simulation consisted of Philbrick Universal Linear Operators, model K5-U, and Philbrick Multiplier-Dividers, model K5-M. The outputs were displayed on a Philbrick Display System, model 5934.

The non-linear mathematical model can be solved for the highest order derivative of the vehicular displacement in terms of the lower order derivatives as

$$\frac{p_{ce}-p_a}{\gamma p_{ce}} \frac{h_e}{g} \dddot{\bar{y}}_2 = \frac{1}{\bar{V}_o + \bar{A}\,\bar{h}} \left[w_e \sqrt{1 - \frac{1}{\delta F} \frac{h_e}{g} \ddot{\bar{y}}_2} - \bar{w}_e \bar{h} \sqrt{1 + \frac{h_e}{g} \ddot{\bar{y}}_2} - \bar{A}\,\dot{\bar{h}} \right] \qquad (41)$$

Using this equation, the operational block diagram can then be built up by using integrators to calculate the lower order derivatives, thus closing the feedback loops and completing the solution. The operational block diagram thus formed, assuming the scaling factor is one volt equals one dimensionless unit, is shown in figure eight (8).

In determining the voltage scaling factor to be used for the actual simulation, there were two major considerations resulting from limitations of the analog computer components.

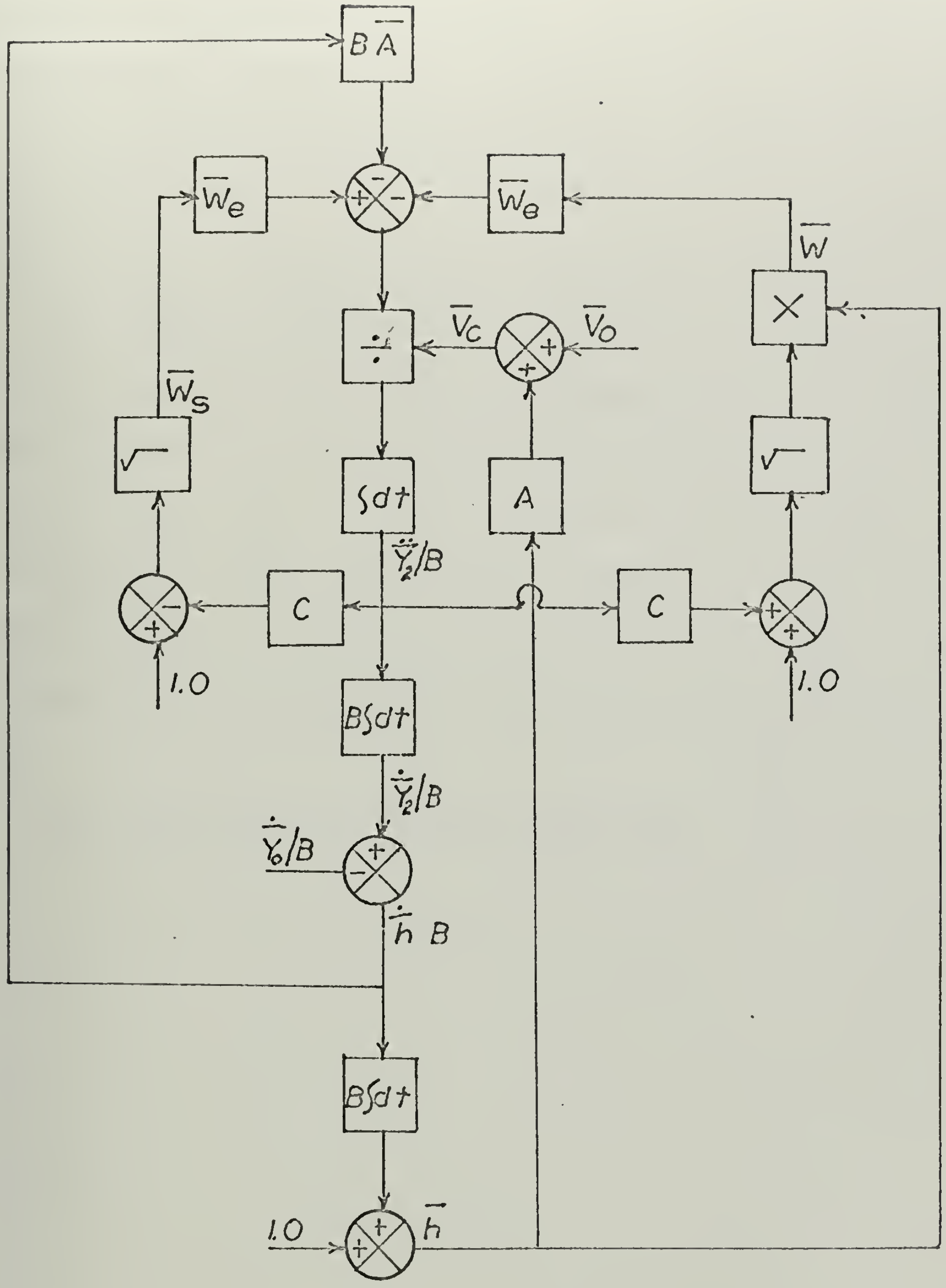

$C = \gamma p_{ce}/(p_{ce}-p_a)$ $B = \sqrt{C(g/h_e)}$

FIGURE 8, Operational Block Diagram of a Simple Rigid Plenum Suspension Assuming a Unity Voltage Scaling Factor

The first consideration involves the fact that the computer dimensionless vehicle acceleration (vehicle acceleration divided by the acceleration due to gravity) is expected to be rather small and therefore near the noise level of the computer. Therefore, the scaling factor should be as high as possible.

The second consideration determines the upper limit, as the computer dimensionless clearance (vehicle clearance height divided by the equilibrium clearance height) could double in magnitude. Thus the scaling factor cannot be too large as this value might then go beyond the maximum operational level of the computer which is fifty volts. Thus a compromise voltage scale of twenty-five volts per dimensionless unit was used.

The time scaling used was real time.

DEVELOPMENT OF DATA POINTS

The computer simulation was used to obtain two sets of data through the use of two different sets of initial conditions.

The first was through the use of the optimum lag time, as determined from figure three (3), for an assumed lead time constant. The remainder of the design parameters of this set of data could then be calculated assuming the following constraints:

1. The ratio of the maximum incremental force to the equilibrium force ($\overline{\delta F}$) is one.
2. The equilibrium clearance (h_e) is one inch.
3. The minimum allowable dimensionless active volume ($\bar{A}$) is 0.1.
4. Only discrete equilibrium cushion pressures (p_{ce}) of 15.2, 15.7, 16.2, and 16.7 psia are used.

Dividing equation five (5) by equation six (6) to obtain

$$\frac{\tau_1'}{\tau_2'} = \bar{A}\,\frac{\gamma p_{ce}}{p_{ce}-p_a}\,\frac{1+1/\overline{\delta F}}{2} \tag{42}$$

it is possible to determine the lowest equilibrium cushion pressure which will satisfy the constraint on the dimensionless

active volume and to then solve for the dimensionless active volume using the next largest discrete value of the equilibrium cushion volume.

The dimensionless dead volume ($\bar{V}_o$) was then calculated from

$$\bar{V}_o = 1 - \bar{A} \tag{43}$$

which can be obtained from equation thirty-five (35) at equilibrium.

The natural frequency (ω_n) can then be calculated from

$$\omega_n = \sqrt{\frac{g}{h_e}} \sqrt{\frac{2}{1+1/\delta F}} \tag{15}$$

Finally, the flow ratio ($\bar{w}_e$) can be determined from

$$\bar{w}_e = \frac{\bar{A}\,\omega_n}{\tau_1'} \tag{44}$$

which can be obtained from combining equations five (5) and thirteen (13).

Using these values, the computer was programed and tested against the linear theory solution using a dimensionless perturbation height of 0.01. If the results corresponded with the linear theory solution, the dimensionless perturbation

height was increased until either the vehicle struck the guideway or the cushion pressure exceeded the source pressure.

The second set of data was obtained in the same manner except that the lead to lag time constant ratio was assumed, thereby determining the lag time constant, rather than using the optimum lag time constant as above.

SUMMARY OF DATA

The following two tables contain the summary of the data used as the basis for figures four (4) through seven (7).

τ_1'	0.04		0.07		0.10	
	$\lvert H_p$	$/A_p$	$\lvert H_p$	$/A_p$	$\lvert H_p$	$/A_p$
Linear	25.0	25.0	15.0	15.0	11.0	10.5
$\bar{y}_o$ = 0.01	24.0	24.0	14.8	14.8	10.8	10.4
0.02	18.0	21.0	14.8	14.8	10.8	10.4
0.04	13.0	15.0	13.0	13.5	10.8	10.4
0.07	9.2	10.8	8.8	9.7	8.0	8.6
0.10			7.2	8.2	6.6	7.4

τ_1'	0.20		0.40		0.70	
	$\lvert H_p$	$/A_p$	$\lvert H_p$	$/A_p$	$\lvert H_p$	$/A_p$
Linear	5.9	5.9	3.4	3.6	2.5	2.9
$\bar{y}_o$ = 0.01	6.0	6.0	3.2	3.6	2.4	2.8
0.02	6.0	6.0	3.2	3.6	2.4	2.8
0.04	6.0	6.0	3.2	3.6	2.4	2.8
0.07	6.0	6.0	3.2	3.6	2.4	2.8
0.10	5.2	5.6	3.2	3.6	2.4	2.8
0.20	3.7	4.2	3.1	3.6	2.4	2.8
0.40					2.1	1.4

TABLE 1, Summary of Data for Various Lead Time Constants

τ'_1/τ'_2	2.0		1.7		1.4	
	|H_p	/A_p	|H_p	/A_p	|H_p	/A_p
Linear	3.0	3.6	3.7	4.2	5.6	6.1
$\bar{y}_o$ = 0.01	3.0	3.6	3.6	4.2	5.5	6.2
0.02	3.0	3.6	3.6	4.2	5.5	6.2
0.04	3.0	3.6	3.6	4.2	5.5	6.2
0.07	3.0	3.6	3.6	4.2	5.5	6.2
0.10	3.0	3.6	3.6	4.2	5.5	6.2
0.20	3.0	3.6	3.6	4.2	5.5	6.2

τ'_1/τ'_2	1.2		1.1		1.0	
	|H_p	/A_p	|H_p	/A_p	|H_p	/A_p
Linear	9.9	10.5	18.5	19.1	∞	∞
$\bar{y}_o$ = 0.01	9.5	11.0	18.0	19.0	50.0	54.0
0.02	9.5	11.0	18.0	19.0	28.0	30.0
0.04	9.5	11.0	14.5	16.0	16.0	17.0
0.07	8.8	10.5	9.7	10.8	10.4	11.1
0.10	7.6	8.4	7.6	8.5	7.6	8.6

TABLE 2, Summary of Data for Various Lead-to-Lag Time Constant Ratio

SAMPLE CALCULATION

$\tau'_1 = 0.4$ (assumed)

$\tau'_2 = 0.1$ (from figure two)

$$\frac{\tau'_1}{\tau'_2} = \frac{0.4}{0.1} = 4.0$$

Determination of the minimum equilibrium cushion pressure

$$\frac{p_{ce}-p_a}{p_{ce}} = \gamma\ \bar{A}\ \frac{\tau'_2}{\tau'_1}\ \frac{1+1/\sqrt{\delta F}}{2}$$

$$\frac{p_{ce}-14.7}{p_{ce}} = (1.4)\ (0.1)\ \frac{0.1}{0.4}\ \frac{1+1}{2} = 0.035$$

$$0.965 p_{ce} = 14.7$$

$$p_{ce} = 15.3 \text{ psia}$$

Therefore, the equilibrium cushion pressure will be 15.7 psia, and

$$\bar{A} = \frac{\tau'_1}{\tau'_2}\ \frac{p_{ce}-p_a}{\gamma p_{ce}}\ \frac{2}{1+1/\sqrt{\delta F}} = \frac{0.4}{0.1}\ \frac{15.7-14.7}{(1.4)(15.7)}\ \frac{2}{1+1} = 0.182$$

$$\bar{V}_o = 1 - \bar{A} = 1 - 0.182 = 0.818$$

$$\omega_n = \sqrt{\frac{g}{h_e}}\sqrt{\frac{2}{1+1/\delta F}} = \sqrt{\frac{32.2}{(1/12)}}\sqrt{\frac{2}{1+1}} = 19.65 \text{ sec}^{-1}$$

$$\bar{W}_e = \frac{A\,\omega_n}{\tau_1'} = \frac{(0.182)(19.65)}{0.4} = 8.94 \text{ sec}^{-1}$$

From figure two (2), the peak dimensionless acceleration and the peak dimensionless change in vehicle-suspension-guideway clearance are:

$$/A_p = 3.6$$

$$|H_p = 3.4$$

For a dimensionless disturbance of $y_o/h_e = 0.01 \text{ Sin}(19.65\ t)$ the observed values are:

$$\frac{|\ddot{y}_2|}{g} = 0.9 \text{ volts} = 0.036$$

$$\frac{|h-h_e|}{h_e} = 0.8 \text{ volts} = 0.032$$

Therefore

$$/A_p = \frac{|\ddot{y}_2|}{y_o\omega_n^2} = \frac{|\ddot{y}_2|}{g}\ \frac{g}{h_e}\ \frac{1}{\omega_n^2}\ \frac{h_e}{y_o} = \frac{(0.036)(386)}{(19.65)^2(0.01)} = 3.6$$

$$\mathrm{IH}_p = \frac{|h-h_e|}{y_o} = \frac{|h-h_e|}{h_e}\,\frac{h_e}{y_o} = \frac{0.032}{0.01} = 3.2$$

BIBLIOGRAPHY

Captain, K. M., Ribich, W. A., and Richardson, H. H., The Dynamics of Fluid Suspended Ground Transportation Vehicles: A First-Order Analysis, an undated report prepared for the U. S. Department of Transportation under contract C-85-65.

Captain, K. M., Ribich, W. A., and Richardson, H. H., Dynamics of Simple Air-Supported Vehicles Operating Over Irregular Guideways, Engineering Projects Laboratory Report No. 76110-4, Massachusetts Institute of Technology, Cambridge, Massachusetts, June 1967, PB 173 655.

"Is This the Short-Haul Craft of the Future?", Naval Engineers Journal, June 1967, Reprinted from Surveyor, February 1967.

Nakonechny, B. V.,"Survey of Present State of Technology and Practical Experience with Air-Cushion Vehicles," Naval Engineers Journal, August 1967.

Ribich, W. A., and Richardson, H. H., Dynamic Analysis of Heave Motion for a Transportation Vehicle Fluid Suspension, Engineering Projects Laboratory Report No. 76110-3, Massachusetts Institute of Technology, Cambridge, Massachusetts, January 1967, PB 173 685.

Wosser, J. L., "New Amphibious Vehicle Program, Part I, Air Cushion Vehicles," Naval Engineers Journal, June 1965.

Kiessel

Investigation of the non-linear characteristics of fluid-suspended vehicles.

Thesis
K398 Kiessel 99298
Investigation of the non-linear characteristics of fluid-suspended vehicles.